




MyD88 in hepatic stellate cells promotes the development of alcoholic fatty liver via the AKT pathway

Yukun Li¹ · Miaomiao Wei¹ · Qi Yuan¹ · Yu Liu¹ · Tian Tian¹ · Lingling Hou¹  · Jinhua Zhang¹

Received: 29 October 2021 / Revised: 22 March 2022 / Accepted: 28 March 2022 / Published online: 16 June 2022
© The Author(s), under exclusive licence to Springer-Verlag GmbH Germany, part of Springer Nature 2022

Abstract

Myeloid differentiation primary response gene 88 (MyD88), an adaptor protein in the Toll-like receptors (TLRs) signalling pathway, is expressed in various liver cells including hepatocytes, Kupffer cells and hepatic stellate cells (HSCs). And yet, the functional role of MyD88 in HSCs is poorly elucidated in alcoholic fatty liver (AFL). Here, to study the functional role of MyD88 in HSCs and the molecular mechanism related to the development of AFL, chronic-binge ethanol mouse models were established in mice with specific MyD88 knockout in quiescent (MyD88^{GFAP-KO}) and activated HSCs (MyD88^{SMA-KO}), respectively. Our results clearly showed an elevated expression of MyD88 in liver tissues of ethanol treated mouse model which harbours the wild type. Intriguingly, ethanol treatment profoundly inhibited inflammation in both MyD88^{GFAP-KO} and MyD88^{SMA-KO} mice, but the suppression of lipogenesis was only observed in MyD88^{GFAP-KO} mice. Molecularly, our study indicated that MyD88 induced osteopontin (OPN) secretion in HSCs, which consequently resulted in activation of AKT signalling pathway and accumulation of fat in hepatocytes. Additionally, our data also suggested that OPN promoted inflammation by activating p-STAT1. Thus, targeting MyD88 may be a potentially represent a promising strategy for the prevention and treatment of AFL.

Key messages

- The expression of MyD88 in HSCs was significantly increased in ethanol-induced liver tissues of wild-type mice.
- MyD88 deficiency in quiescent HSCs inhibited inflammation and lipogenesis under the ethanol feeding condition.
- MyD88 deficiency in activated HSCs only inhibited inflammation under the ethanol feeding condition.
- MyD88 promoted the OPN secretion of HSCs, which further activated the AKT signalling pathway of hepatocytes and upregulated lipogenic gene expression to promote fat accumulation.
- OPN also promotes inflammation by activating p-STAT1.

Keywords MyD88 · Hepatic stellate cells · Alcoholic fatty liver · Osteopontin

Introduction

Alcohol consumption abuse is a leading cause of alcoholic liver disease (ALD), which has been characterized by a wide spectrum of liver pathologies ranging from fatty liver, alcoholic hepatitis, fibrosis, cirrhosis and hepatocellular carcinoma (HCC) [1, 2]. Alcoholic fatty liver (AFL) is the initial stage of the disease, but the accumulated evidence shows that there are potential pathological features [3, 4]. To date, several molecular mechanisms related to hepatic lipid metabolism have been elucidated [5, 6]. Ethanol metabolism-associated oxidative stress and chemokines have been reported to play critical roles in the development of AFL [7, 8]. Although the potential treatments of AFL

Yukun Li and Miaomiao Wei these authors contributed equally to this work.

✉ Lingling Hou
llhou@bjtu.edu.cn

✉ Jinhua Zhang
zhangjh@bjtu.edu.cn

¹ The College of Life Science and Bioengineering, Beijing Jiaotong University, Beijing, People's Republic of China

have been developed for decades, resistance to the traditional therapies still limits their efficacy. Therefore, development of novel targets or strategies for the treatment of AFL seems to be necessary and promising.

AFL is a type of lipid metabolism disorder that mainly manifests as hepatic steatosis. Steatosis is defined as a minimum of 5% intrahepatic fat accumulation in the liver, which is characterized by an increase in triglycerides and cholesterol esters [9]. The increase in lipid synthesis is caused by elevated expression of lipogenic enzymes and cytokines, such as fatty acid synthase (FAS), acyl CoA carboxylase (ACC), ATP citrate lyase (ACL) and malic enzyme (ME). These enzymes and cytokines are regulated by sterol regulatory element binding protein-1c (SREBP-1c), a protein that can be translocated from the nuclear to the cytosol under hepatic ethanol oxidation [10, 11]. Hepatic ethanol oxidation triggers the translocation of SREBP-1c. SREBP-1c is matured by proteolysis and becomes a SREBP protein fragment with transcriptional activity, which enters the nucleus and enhances lipogenic gene expression. Thus, regulation of lipid metabolism can be used as a target for prevention or treatment of fatty liver-related steatosis.

Hepatic stellate cells (HSCs) are a type of non-parenchymal cell in the liver. In a healthy liver, HSCs remain in quiescent status and contain a large number of lipid droplets in which vitamin A is stored [12]. When the liver is damaged, HSCs are activated into myofibroblasts, express α -smooth actin (α -SMA) and secrete various extracellular matrix proteins [13]. HSCs play a role in AFL, hepatitis, liver fibrosis, liver cirrhosis and liver cancer. Activated HSCs can promote liver fibrosis and regenerate liver epithelial cells. In addition, activated HSCs release a variety of growth factors and promote tumour growth [14]. Activated HSCs can also recruit macrophages and promote the secretion of TNF- α , which binds to the corresponding receptors on hepatocytes to induce the expression of fat-related genes. It has also been reported that alcohol stimulates HSCs to produce excessive 2-arachidonoylglycerol (2-AG), which further upregulates the expression of fat-related genes in hepatocytes through the paracrine pathway and facilitates the occurrence of AFL [15]. At present, the mechanism by which HSCs regulate lipogenesis is poorly understood.

Toll-like receptors (TLRs) recognize pathogen-associated molecular patterns (PAMPs) and damage-associated molecular patterns (DAMPs) as dimers and further activate the innate immune system [16, 17]. TLRs are expressed in many different cell types of liver with different expression patterns and play important roles in chronic liver diseases through communication with different cell types. Myeloid differentiation primary response gene 88 (MyD88) is a key adaptor molecule for most TLRs (except TLR3) and IL-1 receptor families and is mainly responsible for transmitting signals to the downstream and activating NF- κ B and MAPK family members, leading to the production of proinflammatory or anti-inflammatory

cytokines and type I interferon [18]. MyD88 plays a critical role in inflammation-related diseases. In addition, it is also involved in the regulation of energy, glucose and lipid metabolism in various cells [19]. The physiological functions of MyD88 varied in different tissues and cell types.

MyD88-dependent signalling in neurons is a key regulator of insulin resistance induced by diet in vivo. It has been reported that MyD88-specific deletion in the central nervous system prevents high fat diet (HFD)-induced peripheral glucose metabolism impairment, palmitate production and blunted insulin resistance [20]. However, systemic knockout of MyD88 exacerbates the impaired glucose tolerance induced by a HFD [21] and increases the risk of diabetes in mice [22]. Specific deletion of MyD88 in hepatocytes leads to glucose intolerance, inflammation and liver insulin resistance independent of body weight and adiposity, which has been verified in the album-MyD88 knockout mice with HFD model, partly due to differences in gene expression and transcription factor activity [23]. Furthermore, MyD88 in endothelial cells and myeloid cells also induces inflammation and insulin resistance in HFD model [24]. Nagy LE et al. found that deficiency of MyD88 in myeloid cells inhibited steatosis and inflammation in a myeloid-specific MyD88-deficient (MyD88^{LysM-KO}) mouse model with Lieber–DeCarli ethanol diet [25]. MyD88 in macrophages (Kupffer cells) promoted ethanol-induced liver injury and steatosis in a HFD model [26]. However, the role and mechanism of MyD88 in HSCs in the occurrence of AFL remain unclear.

For this purpose, mice with MyD88-specific deletion in quiescent HSCs (MyD88^{GFAP-KO}) and activated HSCs (MyD88^{SMA-KO}), respectively, were used to establish a chronic-binge ethanol model to study the role and mechanism of MyD88 in ALD. We found that MyD88 was mainly expressed in HSCs and affected alcohol-induced liver injury and inflammation in a mouse model. MyD88 in quiescent HSCs also promoted hepatic fat accumulation. Further mechanistic studies showed that MyD88 in HSCs promoted liver fat accumulation, mainly by secreting OPN, which resulted in activation of the AKT pathway and upregulation of lipogenic gene expression. Taken together, these results indicated that MyD88 may be a potential candidate for the prevention and treatment of AFL.

Materials and methods

Mice

MyD88^{fllox/fllox} (MyD88^{fl/fl}), GFAP-Cre and SMA-Cre mice on a C57BL/6 background have been previously described [27–30]. Mice with a conditional knockout of MyD88 in GFAP-expressing quiescent HSCs (MyD88^{GFAP-KO}) were

generated by crossing MyD88^{fl/fl} and GFAP-Cre mice. And mice with a conditional knockout of MyD88 in SMA-expressing activated HSCs (MyD88^{SMA-KO}) were generated by crossing MyD88^{fl/fl} and SMA-Cre mice. All mice were bred in specific pathogen-free and humidity- and temperature-controlled microisolator cages with a 12-h light/dark cycle at the Institute of Biophysics Chinese Academy of Sciences. All animal studies were performed after being approved by the Institutional Laboratory Animal Care and Use Committee of the Institute of Biophysics, Chinese Academy of Sciences and College of Science, Beijing Jiaotong University.

Chronic-binge ethanol mouse models

Chronic-binge ethanol mouse models were established as described previously [31]. Eight-week-old male C57BL/6 mice, MyD88^{GFAP-KO} and MyD88^{SMA-KO} mice were fed a liquid control diet (TROPIC, Nantong, China) for 2 days to adapt to a liquid diet and then were randomly divided into two groups (five mice in each group), mice in the ethanol group were fed a liquid Lieber–DeCarli diet (TROPID, Nantong, China) with 1% ethanol for 2 days, then a 2% ethanol diet for 2 days and a 4% ethanol diet for 7 days and finally maintained on a 5% ethanol diet for 10 days, followed by a single gavage dose of 31.5% ethanol (5 g/kg body weight) on the last day. Control mice were fed a pair-fed diet and finally given a single gavage dose gavage of isocaloric dextrin maltose. Mice were always given a gavage in the morning and euthanized 9 h after the gavage. For the ethanol feeding period, the food intake of the ethanol-fed mice was recorded, and the weight-matched control feeding mice were pair-fed with the same volume of the control diet, so that ethanol- and pair-fed mice consumed equal amounts of diet and ingested the same energy. The body weight of the mice was recorded every day.

Cell culture

The LX-2 and HepG2 cell lines were obtained from the American Type Culture Collection (ATCC; Manassas, VA, USA). These cells were cultured in DMEM (BI, Israel) supplemented with 10% foetal bovine serum (FBS, BI) and 1% penicillin/streptomycin at 37 °C with 5% CO₂. In the experimental groups, LX-2 cells were exposed to ST2825 (10 μM) (MedChemExpress, Princeton, NJ, USA) for 2 h and then challenged with TLR1/2 agonist (Pam3CSK4, 100 ng/mL), TLR4 agonist (LPS, 1 mg/mL) or palmitic acid (400 μM) (Sigma, USA), respectively, for 24 h. In the control groups, LX-2 cells were directly challenged with TLR1/2 agonist (Pam3CSK4, 100 ng/mL), TLR4 agonist (LPS, 1 mg/mL) or palmitic acid (400 μM), respectively, for 24 h. To induce excessive lipid accumulation, HepG2 cells were cultured in DMEM medium

with 20 μM AKT inhibitor (CSNpharm, USA) for 24 h and then 400 mM palmitic acid and 200 ng/mL recombinant protein OPN (Cloud-Clone Corp, China) for 24 h [32].

Collection of conditioned media

LX-2 cells were exposed to ST2825 (10 μM) (MedChemExpress, USA) for 2 h and then challenged with 400 μM palmitic acid for 24 h. The supernatant was collected as the conditioned medium (CM).

Isolation of HSCs

Primary HSCs were isolated from livers of eight-week-old mice as previously described [29]. The mice were anaesthetized with 3% ethyl carbamate and treated with phosphate balanced solution and 0.16 mg/mL collagenase I for liver perfusion. The liver was removed, divided into small pieces and was placed in the digestive buffer at 37 °C for 30 min. Filtered cells were centrifuged at 50 × g for 2 min to remove hepatocytes. The remaining non-parenchymal cell (NPC) fraction was collected, washed and isolated using a 10% and 40% Optiprep (Axis-Shield, Scotland) gradient system, respectively [33]. The purity of the HSCs fraction was estimated by the autofluorescence signal. Cell viability was examined via trypan blue exclusion. Both the cell purity and viability were greater than 90%.

Biochemical assays of blood and liver tissues

Blood samples were collected from mice via the eyeball and centrifuged at 3000 rpm for 10 min to obtain serum. The levels of serum alanine aminotransferase (ALT), aspartate aminotransferase (AST), cholesterol (Cho) and triglyceride (TG) were detected by Pony Testing International Group (Beijing, China). Liver tissues were homogenized in cold phosphate-buffered saline (PBS) and centrifuged at 3000 rpm for 10 min to obtain the supernatant, and TG and Cho levels in the supernatant were measured by Pony Testing International Group (Beijing, China).

Histology and immunostaining

Paraffin or cryostat sections of liver tissue were prepared as described previously [34]. The sliced liver paraffin sections were stained with haematoxylin and eosin (H&E) (Zhongshanjinjiao, Beijing, China) and Sirius Red, respectively. To detect hepatic fat accumulation, cryostat liver sections were stained with Oil Red O. For immunofluorescence detection, the cryostat sections were, respectively, incubated with anti-F4/80, anti-Gr-1, anti-CD11b (1:200; BD Pharmingen, San Diego, CA), anti-MyD88 and anti-GFAP (1:200; Abcam, Cambridge, UK) antibodies and followed by incubation with Alexa Fluor 488- or 594-conjugated

secondary antibodies (1:500; Invitrogen, Carlsbad, CA, USA). Eventually, cell nuclei were stained with DAPI. The results were evaluated under a microscope (DP71, OLYMPUS) of both bright-field and fluorescence microscopy.

Quantitative real-time polymerase chain reaction (qRT-PCR)

Total RNA was isolated, respectively, from frozen liver tissues and cells using TRIzol reagent (Invitrogen, USA), and then, up to 0.5 μg of RNA was reverse transcribed using Prime Script RT Master Mix Kit (MedChemExpress, Princeton, NJ, USA). cDNA was duplicated using a SYBR Premix ExTaq™ Kit (MedChemExpress, Princeton, NJ, USA). The primer sequences are listed in Supplementary Table 1. Data were analysed using the $2^{-\Delta\Delta C_t}$ method and normalized to GAPDH expression as previously described [35].

Western blot analysis

Western blotting was performed as previously described [36]. Tissue and cell extracts were separated via electrophoresis on a 10% SDS-PAGE gel at 115 V for 1.2 h and transferred to a PVDF membrane at 200 mA for 1 h. Membranes were blocked with 5% milk in TBST for 1 h and incubated overnight at 4°C with the following primary antibodies: anti-MyD88 (Abcam, Cambridge, UK), anti-AKT, anti-p-AKT, anti-STAT1 and anti-p-STAT1 antibodies (Cell Signalling Technology, USA). HRP-conjugated goat anti-mouse IgG and goat anti-rabbit IgG were used as secondary antibodies. Blots were scanned using a Clinx Science Instrument. All specific bands were quantified with the ImageJ automated Digitizing System.

Quantitative and statistical analysis

All the data are expressed as the means \pm SEM and analysed using GraphPad Prism software. Differences between the two groups were compared using two-tailed unpaired Student's t-test analysis. One-way ANOVA tests with a Bonferroni correction were used for multiple comparisons. For all tests, $p < 0.05$ was considered statistically significant. $p < 0.01$ was considered extremely significant.

Results

MyD88 expression in HSCs is upregulated in the liver of AFL mice

To explore the correlation between the expression of MyD88 in the mouse liver and the development of AFL, C57BL/6 mice were administered ethanol to generate chronic-binge ethanol mouse models. Liver tissues were

harvested after the AFL model was established (Fig. 1a). As shown in Fig. 1b and c, western blotting results showed that the expression of MyD88 was significantly upregulated in the livers of ethanol-fed mice compared with levels in the livers of control mice. MyD88⁺ cells in the liver tissue were further detected by immunofluorescence staining. Consistently, ethanol feeding led to a significant increase in the number of MyD88⁺ cells. Double immunofluorescence staining revealed that most of HSCs (GFAP⁺ cells) in the liver tissue of AFL mice expressed MyD88 (Fig. 1d). These results clearly demonstrate that MyD88 expression in HSCs of WT mice is enhanced under the ethanol feeding condition.

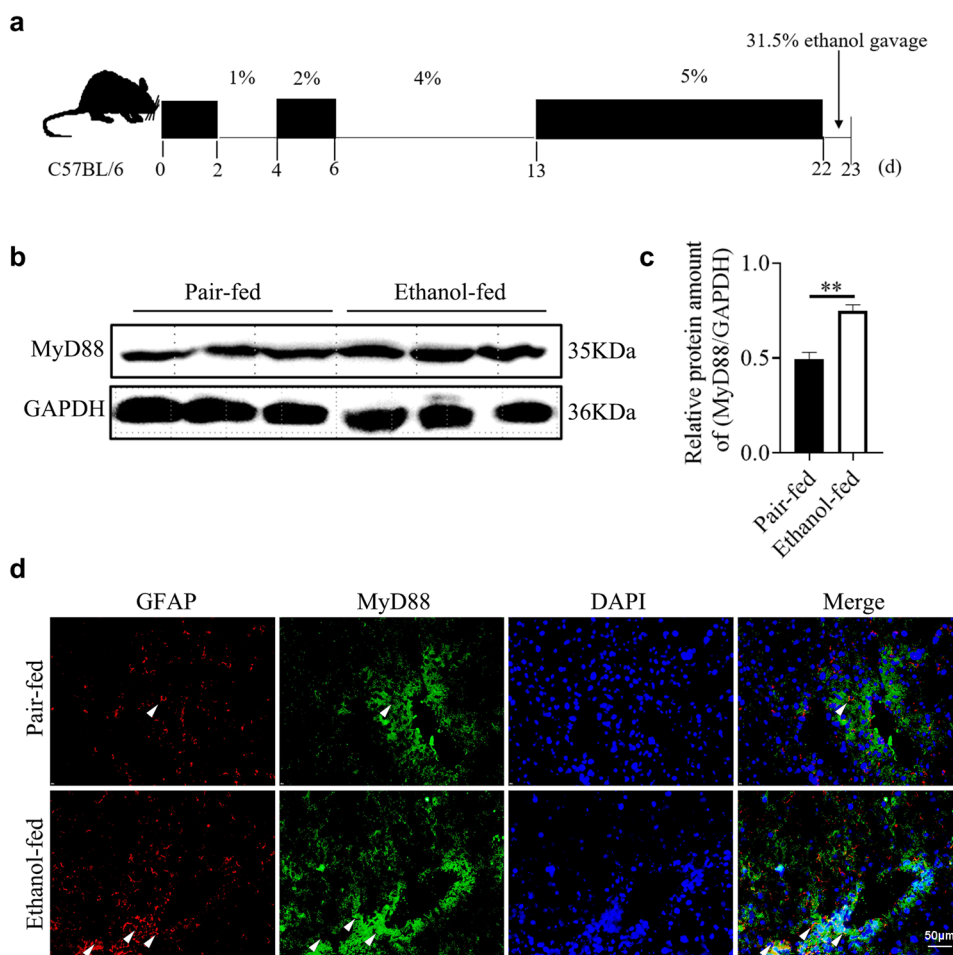
MyD88 deficiency in HSCs attenuates ethanol-induced liver injury

To investigate the contribution of MyD88 in HSCs to liver injury, MyD88^{GFAP-KO} mice, MyD88^{SMA-KO} mice and control littermates were used to establish chronic-binge ethanol models (Supplementary Fig. 1). The results indicated that there was no significant difference in the body weight between MyD88^{GFAP-KO} and MyD88^{fl/fl} mice or between MyD88^{SMA-KO} and MyD88^{fl/fl} mice under the ethanol feeding condition (Fig. 2a, b). To characterize the pathology associated with ethanol feeding in MyD88^{GFAP-KO}, MyD88^{SMA-KO} and MyD88^{fl/fl} mice, liver tissues were collected from each group for further evaluation. We found that MyD88^{GFAP-KO} mice exhibited a higher liver/body weight ratio than MyD88^{fl/fl} mice (Fig. 2c). However, there was no significant difference in the liver/body weight ratio between MyD88^{SMA-KO} mice and MyD88^{fl/fl} mice (Fig. 2d). We further examined the serum ALT and AST levels in MyD88^{fl/fl}, MyD88^{GFAP-KO} and MyD88^{SMA-KO} mice under the ethanol feeding condition. The results demonstrated that both the ALT level in MyD88^{GFAP-KO} mice and the AST level in MyD88^{SMA-KO} mice were dramatically attenuated compared with those levels in MyD88^{fl/fl} mice (Fig. 2e-h). H&E staining also showed that both MyD88^{GFAP-KO} and MyD88^{SMA-KO} mice had weakened inflammatory cell infiltration, hepatocyte cell death and steatosis compared with MyD88^{fl/fl} mice (Fig. 2i, j). Generally, these results confirm that MyD88 knockout in HSCs significantly alleviate liver injury.

MyD88 deficiency in HSCs attenuates ethanol-induced liver inflammation

To investigate the effect of MyD88 in HSCs on inflammation, the infiltration of immune cells was detected by immunofluorescence staining. The results showed that

Fig. 1 Expression of MyD88 is increased in the livers of ethanol-fed mice. C57BL/6 mice ($n=5$ per group) were fed a Lieber–DeCarli liquid diet containing ethanol to establish a chronic-binge ethanol model, and the control group was fed a control liquid diet without ethanol. The expression of MyD88 was detected. **a** Schematic representation of the experimental procedure for construction of the chronic-binge model. **b, c** MyD88 expression in livers was analysed via western blotting and grey values were assessed. $**p < 0.01$. **d** Immunofluorescence staining of MyD88 and GFAP in liver tissues. Nuclei were counterstained with DAPI. The arrows indicate GFAP⁺, MyD88⁺ and GFAP⁺MyD88⁺ cells, respectively. Scale bar = 50 μm



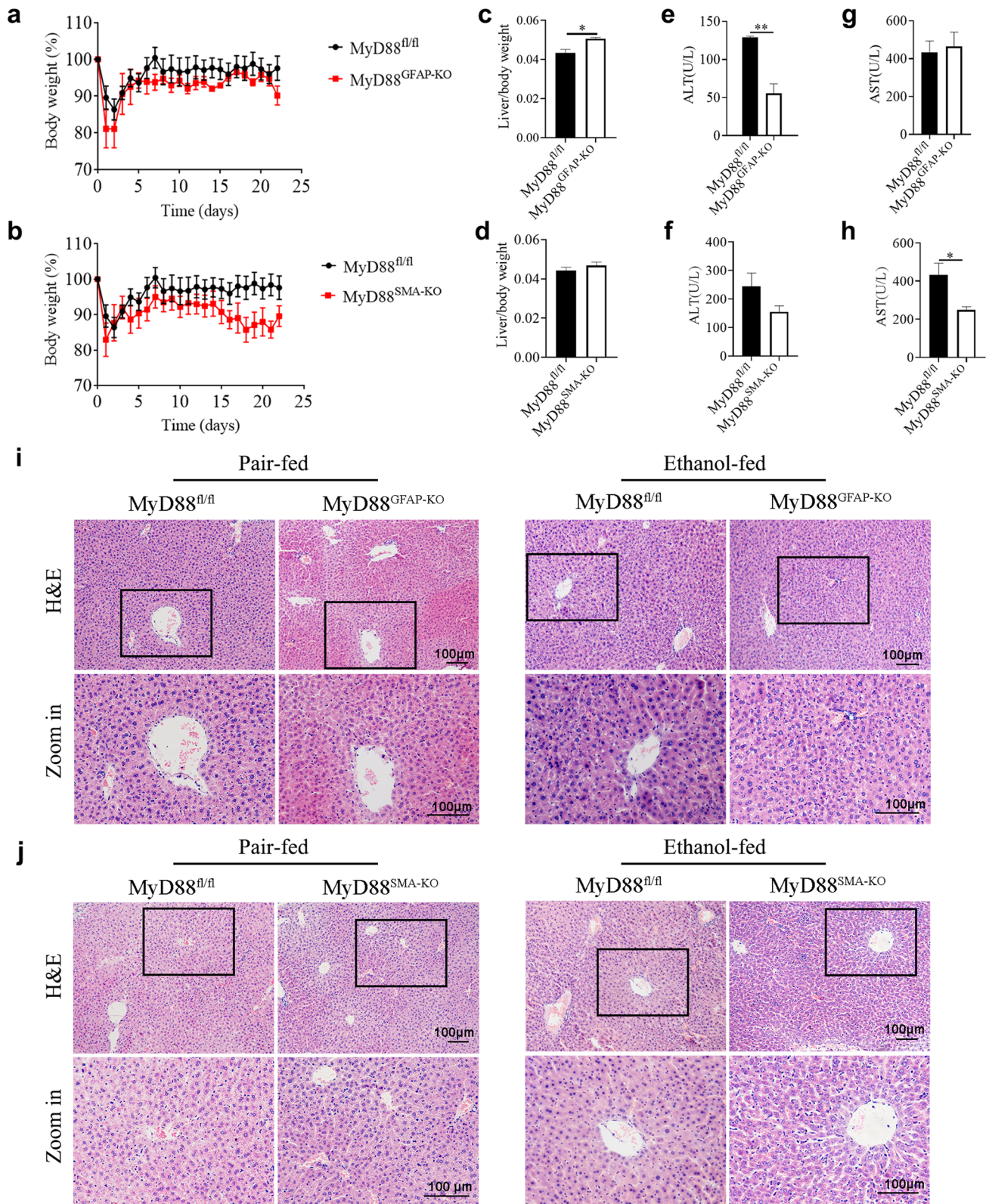
the infiltration of F4/80⁺ macrophages, Gr1⁺ neutrophils and CD11b⁺ monocytes was obviously reduced in MyD88^{GFAP-KO} mice and MyD88^{SMA-KO} mice compared with that in MyD88^{fl/fl} mice under the ethanol feeding conditions (Fig. 3a–d). We further examined the gene expression of proinflammatory cytokines in MyD88^{fl/fl}, MyD88^{GFAP-KO} and MyD88^{SMA-KO} mice, respectively, under the ethanol feeding conditions. As shown in Fig. 3e and f, the mRNA levels of interleukin-6 (IL-6), IL-1 β , tumour necrosis factor α (TNF- α) and monocyte chemoattractant protein-1 (MCP-1) were markedly downregulated in the livers of MyD88^{GFAP-KO} and MyD88^{SMA-KO} mice after ethanol feeding. In summary, these results suggested that MyD88 deletion in HSCs significantly attenuated hepatic inflammation.

MyD88 deficiency in HSCs attenuates fat accumulation

AFL is mainly caused by continuous alcohol intake. The fat in the liver is stored in small lipid droplets in the early stage of steatosis and subsequently expands into large lipid

droplets. Fat accumulation in the liver is often accompanied by elevated Cho and TG. The levels of Cho and TG in mouse serum and liver tissue were detected by biochemical indicators. The results demonstrated that except for serum TG, the levels of serum Cho, hepatic Cho and hepatic TG were all distinctly decreased in the MyD88^{GFAP-KO} mice compared with those levels in MyD88^{fl/fl} mice (Fig. 4a, b). However, there was no significant difference in serum and hepatic TG and Cho between MyD88^{SMA-KO} and MyD88^{fl/fl} mice (Fig. 4c, d).

To further verify the production of TG and other neutral fats in the liver tissue, the liver tissue sections from MyD88^{GFAP-KO}, MyD88^{SMA-KO} and MyD88^{fl/fl} mice were stained with Oil Red O, respectively. As shown in Fig. 4e, the accumulation of lipid droplets in hepatocytes of MyD88^{GFAP-KO} mice was significantly weakened compared with that in MyD88^{fl/fl} mice. Consistently, the mRNA levels of lipogenesis genes such as SREBP1, SCD1, ACC1 and FASN were evidently downregulated in the liver tissues of MyD88^{GFAP-KO} mice compared with levels in MyD88^{fl/fl} mice (Fig. 4f). However, there was no significant difference in hepatic fat accumulation or the expression of lipogenesis



genes between MyD88^{SMA-KO} and control mice (Fig. 4g, h). In addition, the results from Sirius Red staining demonstrated that MyD88 deficiency in quiescent HSCs had no obvious

effects on liver fibrosis in this model (Supplementary Fig. 2). Collectively, these results indicate that MyD88 deficiency in HSCs significantly inhibit the accumulation of hepatic fat.

Fig. 2 MyD88 deficiency in HSCs attenuates ethanol-induced liver injury. Groups of MyD88^{fl/fl}, MyD88^{GFAP-KO} and MyD88^{SMA-KO} mice (n = 5 per group) were fed a Lieber–DeCarli liquid diet containing ethanol to establish a chronic-binge ethanol model, respectively, and the control group was fed a control liquid diet without ethanol. Liver injury was evaluated. **a, b** Changes in the body weight of MyD88^{fl/fl}, MyD88^{GFAP-KO} and MyD88^{SMA-KO} mice. **c, d** Changes in the liver/body weight ratio of MyD88^{fl/fl}, MyD88^{GFAP-KO} and MyD88^{SMA-KO} mice. *p < 0.05. **e–h** Serum ALT and AST levels in mice from different groups. *p < 0.05. **i, j** Representative images of haematoxylin and eosin (H&E) staining of liver tissues in mice from different groups. Scale bar = 100 μm

MyD88 deficiency in quiescent HSCs inhibits the expression of OPN

To study how the MyD88 in quiescent HSCs affects the ethanol-induced inflammation and adipogenesis in liver cells, the GEO database (GSE151158) was used to analyse the gene expression levels in the livers of 21 healthy people and 40 fatty liver patients and found that the expression level of the OPN gene in the livers of fatty liver patients was significantly increased (Fig. 5a). Related evidence has shown that OPN can promote adipogenesis [37]. Thus, the expression of OPN in the livers of MyD88^{GFAP-KO} and MyD88^{fl/fl} mice was detected via RT-qPCR. As shown in Fig. 5b, the expression level of OPN was significantly decreased in the livers of MyD88^{GFAP-KO} mice compared with the level in the livers of MyD88^{fl/fl} mice, and there were no obvious changes in MyD88^{SMA-KO} mice (Fig. 5c). Immunohistochemical staining further confirmed that the OPN expression was also significantly reduced in the livers of MyD88^{GFAP-KO} mice (Fig. 5d).

To explore whether MyD88 deficiency in quiescent HSCs affects the secretion of OPN, the LX-2 HSCs were treated with the MyD88 inhibitor ST2825 for 2 h and then with TLR1/2 and TLR4 agonists for 24 h. The results showed that the agonist treatment promoted the expression of OPN in LX-2 cells, and the OPN expression was markedly inhibited after addition of the MyD88 inhibitor ST2825, and the TLR4 agonist showed the most significant effect (Fig. 5e). The above results suggested that the TLR4 signalling pathway played a key role in regulating the expression of OPN. After the activation of the TLR4 signalling pathway by palmitic acid, the expression of MyD88 and OPN was detected by RT-qPCR. The results indicated that ST2825 dramatically suppressed the expression of MyD88 (Fig. 5f), while palmitic acid significantly promoted the expression of OPN. However, when MyD88 was inhibited by ST2825, the promotive effect of palmitic acid on OPN expression was significantly blocked (Fig. 5g). Overall, the results suggest that the expression of OPN in HSCs is regulated by MyD88.

To further study the effect of OPN secreted by HSCs on the adipogenesis in HepG2 cells, HepG2 cells were incubated with conditioned medium (CM) prepared from LX-2

cells for 24 h. Then, the expression of adipogenic genes was detected. The results indicated that the mRNA levels of SREBP1, SCD1 and FANS in HepG2 cells were obviously upregulated (Fig. 5h). HepG2 cells were treated with palmitic acid to induce fatty liver-like cells, and the expression of lipogenesis genes in HepG2 cells was analysed via RT-qPCR. We found that the expression of SREBP1, SCD1, ACC1 and FANS in HepG2 cells was significantly enhanced (Fig. 5i). Subsequently, recombinant OPN protein was added exogenously to explore its effect on the adipogenesis of HepG2 cells. RT-qPCR results showed that OPN dramatically promoted the expression of SCD1, FANS, SREBP and ACC1 in HepG2 cells (Fig. 5i). In general, these results confirm that OPN secreted by HSCs markedly promotes adipogenesis in HepG2 cells.

MyD88 promoted liver fat accumulation and inflammation via the AKT pathway and STAT1 pathway, respectively

To elucidate the underlying mechanism responsible for ethanol-induced hepatic lipid accumulation, we examined the signalling pathways in which MyD88 may be involved during liver fat accumulation and inflammation. The results showed that there was no significant difference in the total AKT protein level in the liver tissues between MyD88^{GFAP-KO} mice and MyD88^{fl/fl} mice (Fig. 6a), but the p-AKT expression level was noticeably increased in the liver of MyD88^{GFAP-KO} mice compared with that in MyD88^{fl/fl} mice (Fig. 6a, b). Meanwhile, no obvious difference in the total STAT1 protein level in the liver was observed between MyD88^{GFAP-KO} mice and MyD88^{fl/fl} mice, but the phosphorylated STAT1 level in MyD88^{GFAP-KO} mice was much lower than that in MyD88^{fl/fl} mice (Fig. 6a, b). The AKT and STAT1 signalling pathway were further analysed in the human hepatoma cell line HepG2. HepG2 cells were pretreated with palmitic acid for 24 h and then treated with OPN for 24 h. The related protein expression levels of the AKT and STAT1 signalling pathways were analysed via western blotting. The results showed that the phosphorylation level of AKT was distinctly weakened, while the phosphorylation level of STAT1 was significantly enhanced in the OPN treatment group compared with the control group (Fig. 6c, d). To further explore whether OPN affects fat accumulation by regulating the phosphorylation of AKT, we investigated the expression of adipogenesis genes after treatment with the AKT inhibitor MK-2206 in HepG2 cells and found that the expression of the adipogenesis genes SCD1, FANS, SREBP1 and ACC1 was significantly upregulated (Fig. 6e). Collectively, the above results suggest that MyD88 facilitates liver fat accumulation by activating the AKT pathway and promotes inflammation through the STAT1 pathway.

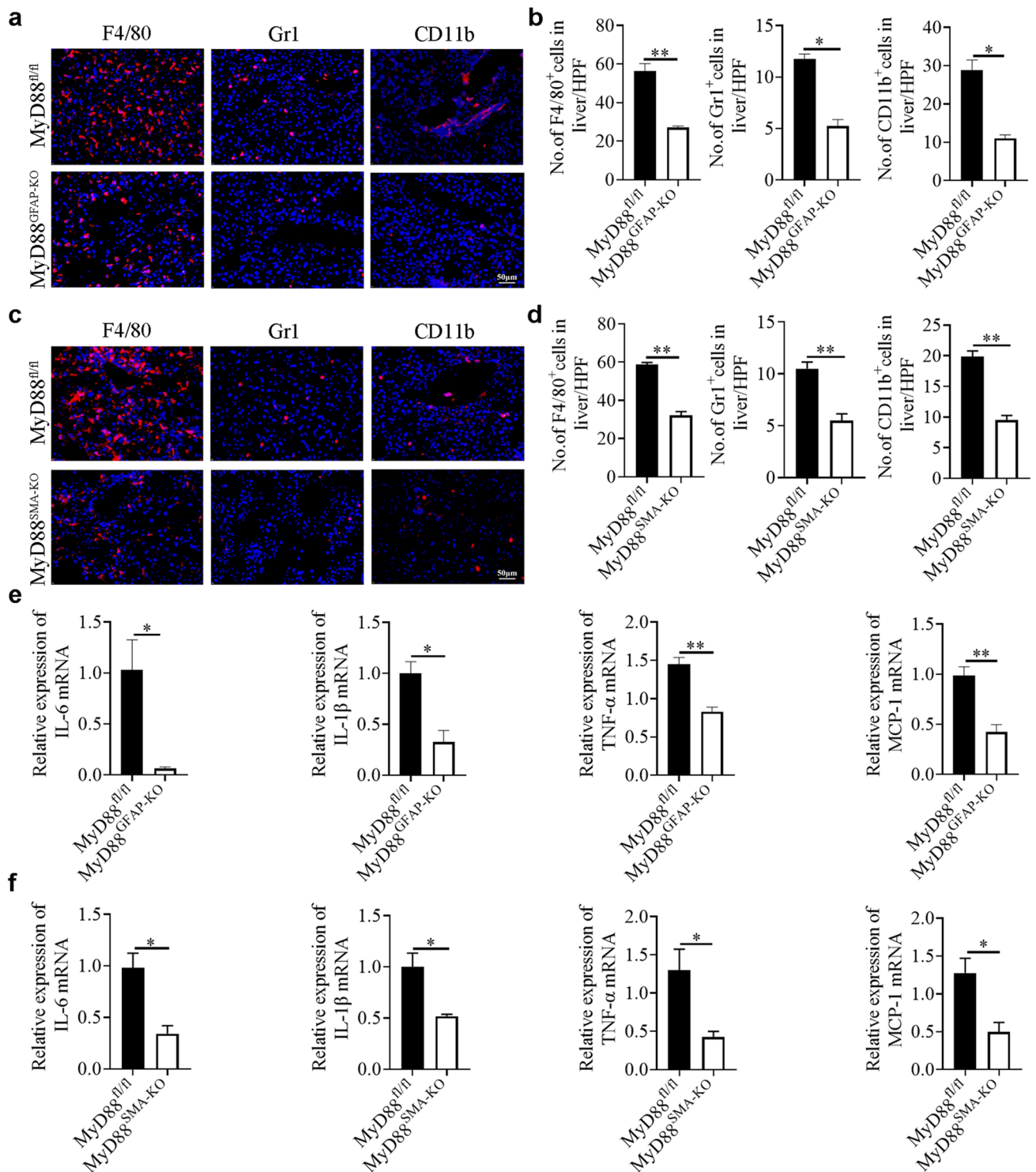


Fig. 3 MyD88 deficiency in HSCs attenuates ethanol-induced liver inflammation. Groups of MyD88^{fl/fl}, MyD88^{GFAP-KO} and MyD88^{SMA-KO} mice (n=5 per group) were fed a Lieber–DeCarli liquid diet containing ethanol to establish a chronic-binge ethanol model, respectively, and the control group was fed a control liquid diet without ethanol. Liver inflammation was analysed. **a**, **c** Immunofluorescence detection of F4/80⁺, Gr-1⁺ and CD11b⁺ cell infiltration in liver tissues of MyD88^{fl/fl}, MyD88^{GFAP-KO} and MyD88^{SMA-KO} mice, respectively. **b**, **d** Representative images and

statistical analysis of immunofluorescence staining for F4/80⁺, Gr-1⁺ and CD11b⁺ infiltration in liver tissues of MyD88^{fl/fl}, MyD88^{GFAP-KO} and MyD88^{SMA-KO} mice. HPF: high-power field. *p<0.05, **p<0.01. Scale bar=50 μm. **e** IL-6, IL-1β, TNF-α and MCP-1 mRNA levels were detected in the liver tissues of MyD88^{fl/fl} and MyD88^{GFAP-KO} mice using real-time PCR method. *p<0.05, **p<0.01. **f** IL-6, IL-1β, TNF-α and MCP-1 mRNA levels in the liver tissues of MyD88^{fl/fl} and MyD88^{SMA-KO} mice were evaluated using real-time PCR method. *p<0.05

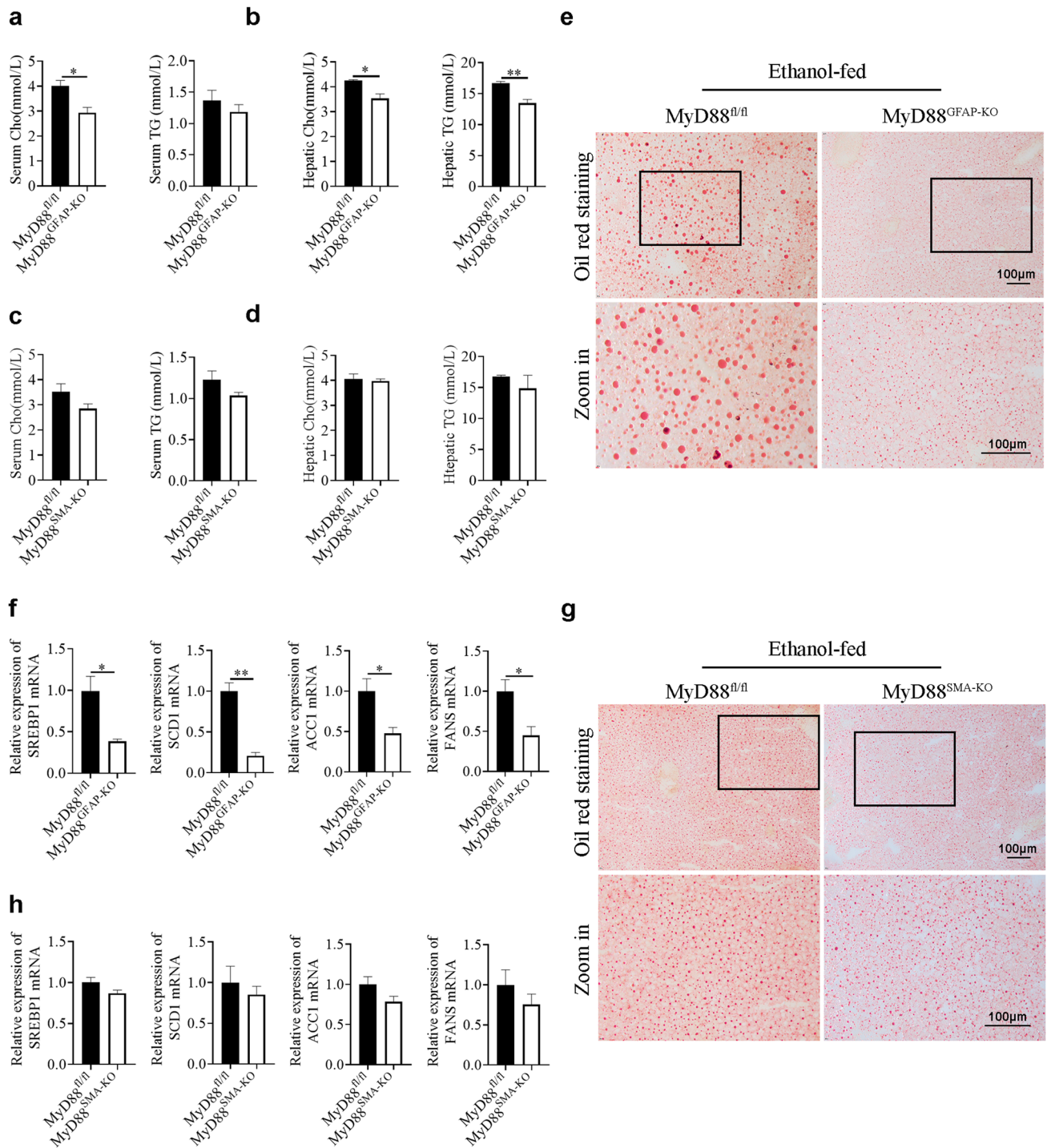
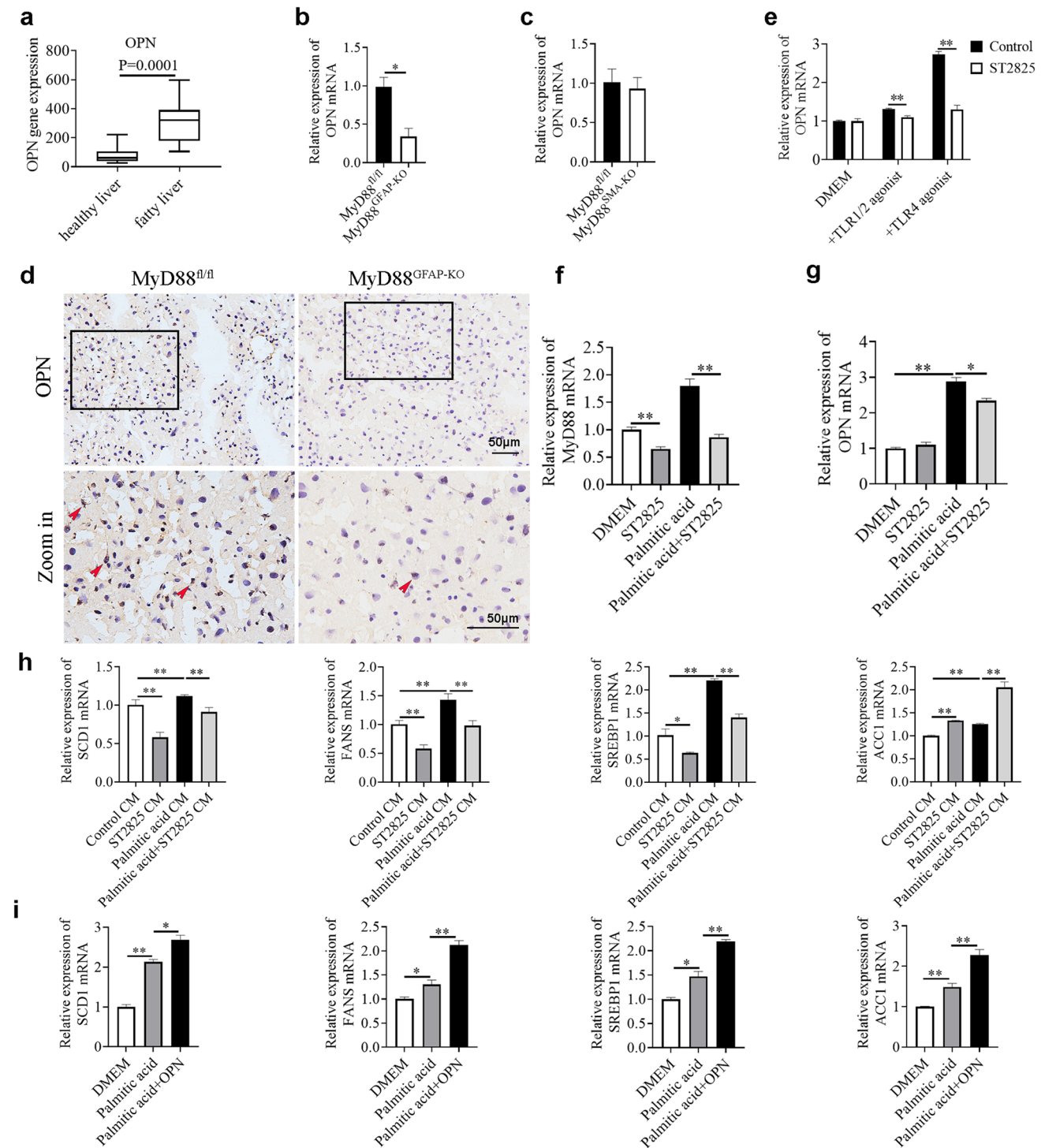


Fig. 4 MyD88 deficiency in quiescent HSCs attenuates liver fat accumulation. Groups of MyD88^{fl/fl}, MyD88^{GFAP-KO} and MyD88^{SMA-KO} mice (n=5 per group) were fed a Lieber–DeCarli liquid diet containing ethanol to establish a chronic-binge ethanol model, respectively, and the control group was fed a control liquid diet without ethanol. Liver fat was analysed. **a** Serum cholesterol (Cho) and triglyceride (TG) levels in MyD88^{fl/fl} and MyD88^{GFAP-KO} mice were detected. **b** Hepatic Cho and TG levels in MyD88^{fl/fl} and MyD88^{GFAP-KO} mice

were tested. *p<0.05, **p<0.01. **c** Serum Cho and TG levels in MyD88^{fl/fl} and MyD88^{SMA-KO} mice were detected. **d** Hepatic Cho and TG levels in MyD88^{fl/fl} and MyD88^{SMA-KO} mice were evaluated. **e, g** Oil red O staining of liver tissues of MyD88^{fl/fl}, MyD88^{GFAP-KO} and MyD88^{SMA-KO} mice, respectively. Scale bar=100 μ m. **f, h** SREBP1, SCD1, ACC1 and FANS mRNA levels in the livers of MyD88^{fl/fl}, MyD88^{GFAP-KO} and MyD88^{SMA-KO} mice were measured using real-time PCR method. *p<0.05, **p<0.01



Discussion

MyD88 is a key player in ALD. However, due to its wide expression, the cell-type-specific contribution of MyD88-mediated signalling to ALD is still unclear. In this study, the role of MyD88 in HSCs was investigated in AFL. We

found that MyD88 deficiency in quiescent HSCs significantly reduced liver injury, inflammation and steatosis, while MyD88 deficiency in activated HSCs (myofibroblasts) only inhibited the progression of liver injury and inflammation, and had no obvious effects on steatosis. Furthermore, mechanistic studies showed that MyD88 was able to activate

Fig. 5 MyD88 deficiency in HSCs downregulates OPN expression. **a** The GEO database was used to analyse the expression level of OPN in the livers of healthy and fatty liver patients. **b, c** Groups of MyD88^{fl/fl}, MyD88^{GFAP-KO} and MyD88^{SMA-KO} mice (n=5 per group) were used to establish the chronic-binge ethanol models. The mRNA levels of OPN in the livers of MyD88^{fl/fl}, MyD88^{GFAP-KO} and MyD88^{SMA-KO} mice were measured using real-time PCR. *p<0.05. **d** Immunohistochemical detection of OPN in liver tissues of MyD88^{fl/fl} and MyD88^{GFAP-KO} mice. Scale bar=50 μm. **e** LX-2 cells were treated with the MyD88 inhibitor ST2825 for 2 h and then were treated with TLR1/2 and TLR4 agonists for 24 h. The mRNA levels of OPN were measured using real-time PCR. **p<0.01. **f, g** LX-2 cells were exposed to ST2825 for 2 h and then were challenged with palmitic acid (400 μM) for 24 h. The mRNA levels of MyD88 and OPN in LX-2 cells were detected using real-time PCR. *p<0.05, **p<0.01. **h** HepG2 cells were incubated with CM prepared from LX-2 cells for 24 h. SREBP1, SCD1 and FANS mRNA levels in HepG2 cells were detected. *p<0.05, **p<0.01. **i** HepG2 cells were treated with palmitic acid for 24 h and then with 200 ng/mL recombinant OPN protein for 24 h, and SCD1, FANS, SREBP1 and ACC1 mRNA levels in HepG2 cells were evaluated using real-time PCR. *p<0.05, **p<0.01

AKT signalling pathways in hepatocytes by regulating OPN secretion from HSCs, which subsequently upregulated the expression of lipogenic genes and further promoted fat accumulation (Fig. 7). Thus, MyD88 may represent a potential target for the prevention and treatment of AFL.

Accumulating evidence has shown that TLRs mediate the innate immune response and are involved in liver injury, inflammation, liver fibrosis and hepatic lipid metabolism, which in return is attributed to the expression of TLRs in a variety of liver cells, including liver parenchymal cells, Kupffer cells, sinusoidal endothelial cells, HSCs, bile duct epithelial cells and liver dendritic cells [38–40]. TLRs other than TLR3 can bind to corresponding ligands and transmit signals through the adapter molecule MyD88, thereby activating the NF-κB and JNK signalling pathways [18]. In this study, we also confirmed the relevance between TLR and liver lipogenesis. We found that MyD88 deficiency in HSCs attenuated ethanol-induced liver inflammation and fat accumulation, and the MyD88/TLR4 signalling pathway played a key role in regulating the expression of OPN and was correlated with the formation of AFL. Nagy LE et al. reported that specific MyD88 deletion in myeloid cells reduced ethanol-induced increases in the plasma ALT level and hepatic steatosis. Ethanol-induced inflammation and the expression of proinflammatory mediators were also attenuated in the livers of MyD88^{LysM-KO} mice [25]. However, Cani PD et al. found that MyD88 deletion in hepatocytes induced profound changes in glucose and lipid metabolism, which specifically shows that the liver glycogen and the phosphorylation of insulin-induced AKT decreased, and that liver lipids and the inflammation in visceral adipose tissue increased [41]. These studies indicated that MyD88 in hepatocytes, myeloid cells and HSCs may have different effects on hepatic steatosis and inflammation and exert these effects through different mechanisms.

In recent years, it has been found that both innate and adaptive immunity are involved in the development of AFL. As pattern recognition receptors, TLRs play a key role in activation of the immune system [42]. As an important adaptor protein in the TLR signalling pathway, MyD88 can not only regulate the immune response but also affect the metabolic processes. Various cell types are involved in the occurrence of AFL, such as hepatocytes, immune cells and HSCs. Among them, Kupffer cells are the most widely studied and cause inflammation, liver damage and fatty liver by secreting a large number of inflammatory cytokines such as TNF-α, IL-1 and IL-17 [43]. Moreover, HSCs not only play a role in the development of liver fibrosis by secreting extracellular matrix, but also promote lipogenesis by secreting factors such as endocannabinoids. Based on these results, we explored the role and mechanism of MyD88 in HSCs in the development of AFL. Our results demonstrate that MyD88 in HSCs promotes lipid accumulation and inflammation via the AKT and STAT1 pathways. MyD88 deficiency in quiescent HSCs significantly suppresses ethanol-induced hepatic lipid accumulation, liver injury and inflammation by inhibiting the secretion of OPN. Thus, MyD88 could be a potential target for AFL therapy.

OPN is a highly phosphorylated glycoprotein that is widely present in the extracellular matrix, has important functions in cardiovascular disease, cancer, diabetes, cell viability and wound healing [44], and is also involved in the immunity regulation, metabolism and inflammation process [41]. In the present study, we found that OPN derived from HSCs acted on hepatocytes and promoted lipogenesis and inflammatory response by inhibiting the phosphorylation of AKT and increasing the phosphorylation of STAT1. Meanwhile, the relevance between OPN and hepatic lipogenesis has also been verified in clinical trials. In the present study, gene expression levels in 21 healthy people and 40 patients with fatty liver were analysed using the GEO database (GSE151158). OPN expression was found to be significantly upregulated in the livers of patients with fatty liver. Consisted with our results, Smid V et al. reported that OPN promoted lipogenesis and might be a potential marker of fatty liver [45]. Moreover, Haber PS et al. confirmed that OPN was overexpressed in the liver of patients with AFL, especially when HSCs were activated, and the expression of OPN was obviously enhanced [46]. Additionally, by constructing OPN-knockout mice and a chronic-binge ethanol model, Morales-Ibanez et al. found that OPN deficiency inhibited liver damage [41]. Gómez-Ambrosi J et al. reported that OPN deficiency prevented hepatic steatosis by decreasing the expression of molecules involved in the onset of fat accumulation such as Pparg, Srebf1, Fasn, Mogat1, Dgat2 and Cidec in OPN-knockout mice with a HFD [47]. Furthermore, related evidence has confirmed that OPN participates in the AKT and STAT1 signalling pathways and plays a role

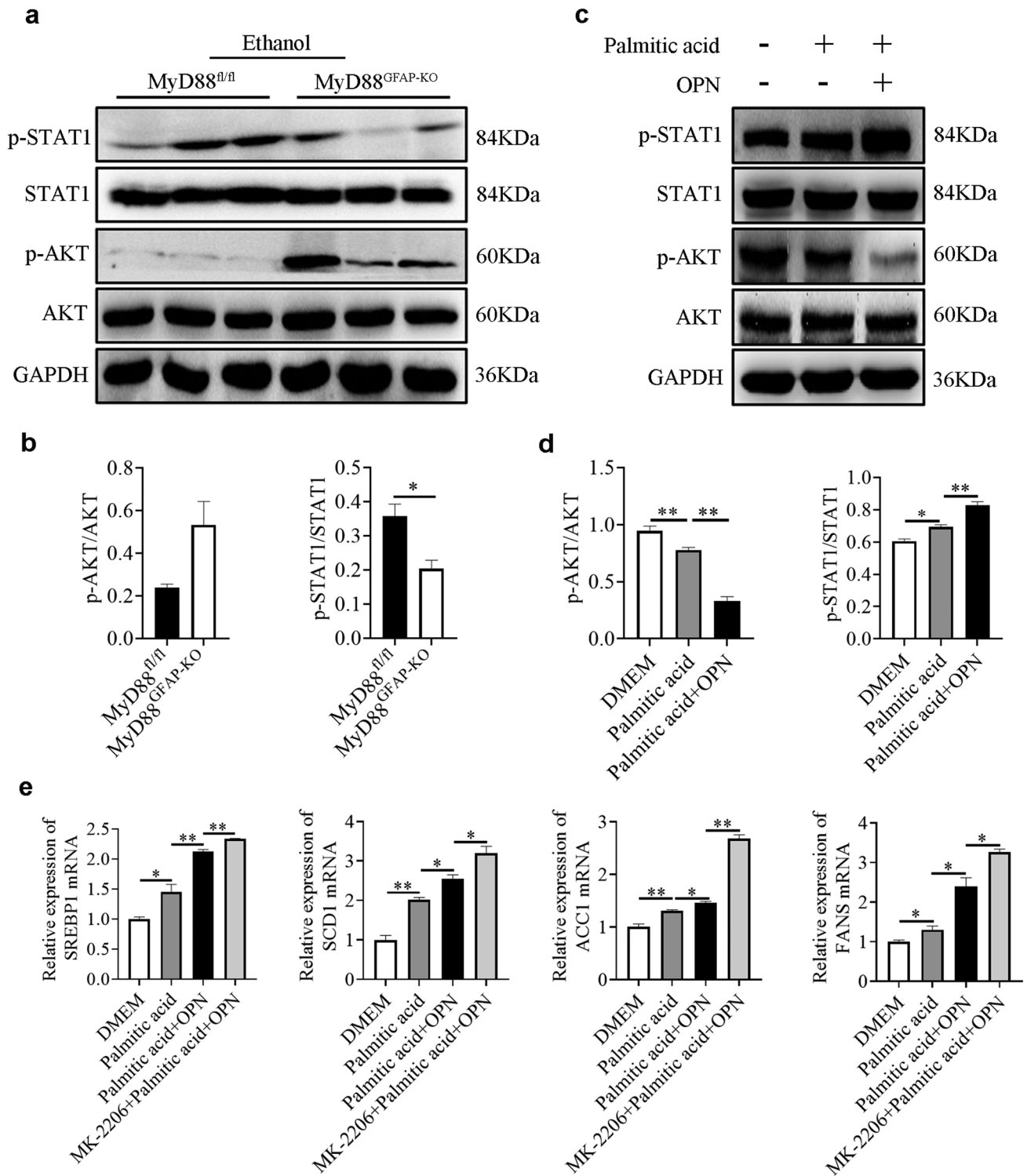
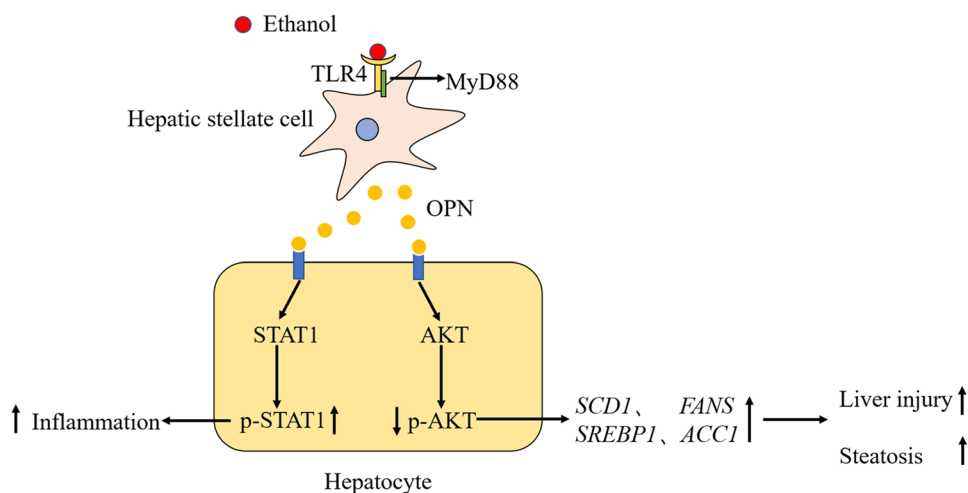


Fig. 6 MyD88 in HSCs promotes liver fat accumulation and inflammation via the AKT pathway and STAT1 pathway, respectively. The mechanism by which MyD88 in HSCs promoted liver fat accumulation and inflammation. **a, b** The protein levels of AKT, p-AKT, STAT1 and p-STAT1 in livers were determined via western blotting. The protein densities were quantified using densitometry. Phosphoprotein levels were normalized to total protein levels. * $p < 0.05$. **c, d** HepG2 cells were treated with 400 μM palmitic acid for 24 h and then with

200 ng/mL recombinant OPN protein for 24 h. The protein levels of AKT, p-AKT, STAT1 and p-STAT1 in HepG2 cells were determined via western blotting. Phosphoprotein levels were normalized to total protein levels. * $p < 0.05$, ** $p < 0.01$. **e** HepG2 cells were treated with palmitic acid for 24 h and then with OPN and the AKT inhibitor MK-2206 for 24 h. The mRNA levels of SREBP1, SCD1, ACC1 and FANS in HepG2 cells were measured using real-time PCR. The results were normalized to GAPDH. * $p < 0.05$, ** $p < 0.01$

Fig. 7 Schematic diagram of the mechanism by which MyD88 in quiescent HSCs promotes adipogenesis and inflammation. Ethanol activated the MyD88-dependent TLR4 signalling pathway in quiescent HSCs, thereby promoting the secretion of OPN in quiescent HSCs. The secreted OPN acted on AKT in HepG2 cells, inhibited the phosphorylation of AKT and further promoted adipogenesis and liver injury. In addition, the secreted OPN also promoted the phosphorylation of STAT1 in HepG2 cells and played a role in promoting inflammation



in steatosis and inflammation. However, GE et al. confirmed that OPN combined with lipopolysaccharide (LPS) reduced the activation of macrophages and the expression of TNF- α , thereby attenuating liver damage and steatosis [48]. The mechanism of OPN in liver injury and steatosis still needs to be further explored.

AFL has become a severe issue that threatens human health worldwide [49]. At present, abstinence, nutritional support and glucocorticoid therapy are still the main methods for the treatment of AFL, and these approaches have various limitations; thus, effective targeted therapy is urgently needed. A deep understanding of the mechanism of AFL is essential and would provide a theoretical and experimental basis for treatment of AFL [50]. The metabolism of ethanol in human body is a complex process. Metabolism of ethanol occurs mainly in the liver via the predominant oxidative metabolism pathway involving phase I enzymes including alcohol dehydrogenases (ADH), cytochrome P450 (CYP) 2E1 and catalase [51]. Besides the oxidative pathway, more and more studies have found that non-oxidative metabolism also plays an important role in ethanol metabolism [52, 53]. Ethanol undergoes metabolism through the non-oxidative pathway generating fatty acid ethyl esters (FAEE), phosphatidylethanol (PEth), ethylsulfate (EtS) and ethylglucuronide (EtG) [54]. Although FAEE are minor metabolites of ethanol, they are formed in almost all tissues after alcohol consumption. This pathway is an enzyme-mediated esterification of fatty acid or fatty acyl-CoA and ethanol. Given the sensitivity and specificity, EtG and EtS in hair and biological fluids are often used as reliable markers of ethanol consumption for clinical use and forensic medicine [53]. FAEE may be hydrolysed to ethanol and fatty acid by FAEE hydrolases. Human hepatocytes in primary culture are considered as a suitable *in vitro* model to study hepatic metabolism of xenobiotics. However, hepatocytes isolated from patients present

important differences in metabolic activities and lose their phenotype over time. Therefore, studies often combined different animal models and human hepatoma cell lines [54]. In this study, HepG2 cell line was used as cell model. HepG2 cells were treated with palmitic acid to mimic the influx of excess FFAs into hepatocytes, palmitic acid can significantly up-regulate the expression of adipogenic genes and induce the rapid accumulation of fat in cells. It was reported that HepG2 cells did not express ethanol-metabolizing enzymes [55, 56], so we speculate that HepG2 cells may metabolize ethanol to accumulate fat through non-oxidative pathways.

Supplementary information The online version contains supplementary material available at <https://doi.org/10.1007/s00109-022-02196-1>.

Acknowledgements Special thanks to Dr. Mengwu Pan (Karlsruhe Institute of Technology) for revising and polishing the language in the manuscript.

Author contributions Jinhua Zhang, Lingling Hou and Yukun Li designed the study; Yukun Li, Miaomiao Wei, Qi Yuan and Yu Liu carried out the experiments; Yukun Li and Miaomiao Wei analysed and interpreted the data. Tian Tian contributed to the discussion of the manuscript. Yukun Li, Lingling Hou and Jinhua Zhang wrote the manuscript. All authors have read and agreed to the published version of the manuscript.

Funding This work was supported by the National Natural Science Foundation of China (81972689 and 81772497).

Data availability statement All relevant data are presented in the paper.

Declarations

Ethical approval All animal studies were performed with the approval of the Institutional Laboratory Animal Care and Use Committee of the Institute of Biophysics, Chinese Academy of Sciences.

Informed consent statement Not applicable.

Research involving human and animal participants All human studies have been approved by the appropriate ethics committee. All animal experiment protocols in the manuscript “MyD88 in hepatic stellate cells promotes the development of alcoholic fatty liver via the AKT pathway” (ID: JMME-D-21-00496R2) were approved by the Institutional Laboratory Animal Care and Use Committee of School of Science, Beijing Jiaotong University.

Conflict of interests The authors declare no conflicts of interest.

References

- Kong LZ, Chandimali N, Han YH, Lee DH, Kim JS, Kim SU et al (2019) Pathogenesis, Early Diagnosis, and Therapeutic Management of Alcoholic Liver Disease. *Int J Mol Sci* 20(11):2712
- Mathurin P, Bataller R (2015) Trends in the management and burden of alcoholic liver disease. *J Hepatol* 62(1 Suppl):S38–46
- Louvet A, Mathurin P (2015) Alcoholic liver disease: mechanisms of injury and targeted treatment. *Nat Rev Gastroenterol Hepatol* 12(4):231–242
- Osna NA, Donohue Jr TM, Kharbanda KK (2017) Alcoholic Liver Disease: Pathogenesis and Current Management. *Alcohol Res* 38(2):147–161
- Gao B, Bataller R (2011) Alcoholic liver disease: pathogenesis and new therapeutic targets. *Gastroenterology* 141(5):1572–1585
- Nagy LE, Ding WX, Cresci G, Saikia P, Shah VH (2016) Linking Pathogenic Mechanisms of Alcoholic Liver Disease With Clinical Phenotypes. *Gastroenterology* 150(8):1756–1768
- Chang B, Xu MJ, Zhou Z, Cai Y, Li M, Wang W et al (2015) Short- or long-term high-fat diet feeding plus acute ethanol binge synergistically induce acute liver injury in mice: an important role for CXCL1. *Hepatology* 62(4):1070–1085
- You M, Jogasuria A, Lee K, Wu J, Zhang Y, Lee YK et al (2017) Signal Transduction Mechanisms of Alcoholic Fatty Liver Disease: Emerging Role of Lipin-1. *Curr Mol Pharmacol* 10(3):226–236
- Gu J, Zhang Y, Xu D, Zhao Z, Zhang Y, Pan Y et al (2015) Ethanol-induced hepatic steatosis is modulated by glycogen level in the liver. *J Lipid Res* 56(7):1329–1339
- Choi YJ, Shin HS, Choi HS, Park JW, Jo I, Oh ES et al (2014) Uric acid induces fat accumulation via generation of endoplasmic reticulum stress and SREBP-1c activation in hepatocytes. *Lab Invest* 94(10):1114–1125
- Greuter T, Malhi H, Gores GJ, Shah VH (2017) Therapeutic opportunities for alcoholic steatohepatitis and nonalcoholic steatohepatitis: exploiting similarities and differences in pathogenesis. *JCI Insight* 2(17):e95354
- de Oliveira da Silva B, Ramos LF, Moraes KCM (2017) Molecular interplays in hepatic stellate cells: apoptosis, senescence, and phenotype reversion as cellular connections that modulate liver fibrosis. *Cell Biol Int* 41(9):946–959
- Shang L, Hosseini M, Liu X, Kisseleva T, Brenner DA (2018) Human hepatic stellate cell isolation and characterization. *J Gastroenterol* 53(1):6–17
- Yin C, Evason KJ, Asahina K, Stainier DY (2013) Hepatic stellate cells in liver development, regeneration, and cancer. *J Clin Invest* 123(5):1902–1910
- Choi WM, Kim HH, Kim MH, Cinar R, Yi HS, Eun HS et al (2019) Glutamate Signaling in Hepatic Stellate Cells Drives Alcoholic Steatosis. *Cell Metab* 30(5):877–89 e7
- Bob J, Ignacio TJA, Esser-Kahn AP, Verdoes M (2018) Toll-like Receptor Agonist Conjugation: A Chemical Perspective. *Bioconjug Chem* 29(3):587–603
- Tamtaji OR, Mobini M, Reiter RJ, Azami A, Gholami MS, Asemi Z (2019) Melatonin, a toll-like receptor inhibitor: Current status and future perspectives. *J Cell Physiol* 234(6):7788–7795
- Deguine J, Barton GM (2014) MyD88: a central player in innate immune signaling. *F1000Prime Rep* 6:97
- Duparc T, Plovier H, Marrachelli VG, Van Hul M, Essaghir A, Stahlman M et al (2017) Hepatocyte MyD88 affects bile acids, gut microbiota and metabolome contributing to regulate glucose and lipid metabolism. *Gut* 66(4):620–632
- Kleinridders A, Schenten D, Konner AC, Belgardt BF, Mauer J, Okamura T et al (2009) MyD88 signaling in the CNS is required for development of fatty acid-induced leptin resistance and diet-induced obesity. *Cell Metab* 10(4):249–259
- Charlotte Lefort MVH, Delzenne NM, Everard A, Cani PD (2019) Hepatic MyD88 regulates liver inflammation by altering synthesis of oxysterols. *Am J Physiol Endocrinol Metab* 317(1):E99–E108
- Bollyky PL, Bice JB, Sweet IR, Falk BA, Gebe JA, Clark AE et al (2009) The toll-like receptor signaling molecule Myd88 contributes to pancreatic beta-cell homeostasis in response to injury. *PLoS One* 4(4):e5063
- Wen L, Ley RE, Volchkov PY, Stranges PB, Avanesyan L, Stonebraker AC et al (2008) Innate immunity and intestinal microbiota in the development of Type 1 diabetes. *Nature* 455(7216):1109–1113
- Everard A, Geurts L, Caesar R, Van Hul M, Matamoros S, Duparc T et al (2014) Intestinal epithelial MyD88 is a sensor switching host metabolism towards obesity according to nutritional status. *Nat Commun* 5:5648
- Zhou H, Yu M, Roychowdhury S, Sanz-Garcia C, Pollard KA, McMullen MR et al (2017) Myeloid-MyD88 Contributes to Ethanol-Induced Liver Injury in Mice Linking Hepatocellular Death to Inflammation. *Alcohol Clin Exp Res* 41(4):719–726
- Hosoi T, Yokoyama S, Matsuo S, Akira S, Ozawa K (2010) Myeloid differentiation factor 88 (MyD88)-deficiency increases risk of diabetes in mice. *PLoS One* 5(9):e12537
- Grcevic D, Pejda S, Matthews BG, Repic D, Wang L, Li H et al (2012) In vivo fate mapping identifies mesenchymal progenitor cells. *Stem Cells* 30(2):187–196
- Vlantis K, Polykratis A, Welz PS, van Loo G, Pasparakis M, Wullaert A (2016) TLR-independent anti-inflammatory function of intestinal epithelial TRAF6 signalling prevents DSS-induced colitis in mice. *Gut* 65(6):935–943
- Yuan Q, Gu J, Zhang J, Liu S, Wang Q, Tian T et al (2021) MyD88 in myofibroblasts enhances colitis-associated tumorigenesis via promoting macrophage M2 polarization. *Cell Rep* 34(5):108724
- Garcia AD, Doan NB, Imura T, Bush TG, Sofroniew MV (2004) GFAP-expressing progenitors are the principal source of constitutive neurogenesis in adult mouse forebrain. *Nat Neurosci* 7(11):1233–1241
- McCullough RL, McMullen MR, Das D, Roychowdhury S, Strainic MG, Medof ME et al (2016) Differential contribution of complement receptor C5aR in myeloid and non-myeloid cells in chronic ethanol-induced liver injury in mice. *Mol Immunol* 75:122–132
- Orlicky DJ, Roede JR, Bales E, Greenwood C, Greenberg A, Petersen D et al (2011) Chronic ethanol consumption in mice alters hepatocyte lipid droplet properties. *Alcohol Clin Exp Res* 35(6):1020–1033
- Weiskirchen S, Tag CG, Sauer-Lehnen S, Tacke F, Weiskirchen R (2017) Isolation and Culture of Primary Murine Hepatic Stellate Cells. *Methods Mol Biol* 1627:165–191
- Hou S, Jiao Y, Yuan Q, Zhai J, Tian T, Sun K et al (2018) S100A4 protects mice from high-fat diet-induced obesity and inflammation. *Lab Invest* 98(8):1025–1038
- Xiayu Rao XH, Zhou Z, Lin X (2013) An improvement of the 2^{-ΔΔCT} method for quantitative real-time polymerase chain reaction data analysis. *Biostat Bioinforma Biomath* 3(3):71–85

36. Yuan Q, Hou S, Zhai J, Tian T, Wu Y, Wu Z et al (2019) S100A4 promotes inflammation but suppresses lipid accumulation via the STAT3 pathway in chronic ethanol-induced fatty liver. *J Mol Med (Berl)* 97(10):1399–1412
37. Kiefer FW, Neschen S, Pfau B, Legerer B, Neuhofer A, Kahle M et al (2011) Osteopontin deficiency protects against obesity-induced hepatic steatosis and attenuates glucose production in mice. *Diabetologia* 54(8):2132–2142
38. Mohs A, Kuttkat N, Otto T, Youssef SA, De Bruin A, Trautwein C (2020) MyD88-dependent signaling in non-parenchymal cells promotes liver carcinogenesis. *Carcinogenesis* 41(2):171–181
39. Roh YS, Seki E (2013) Toll-like receptors in alcoholic liver disease, non-alcoholic steatohepatitis and carcinogenesis. *J Gastroenterol Hepatol* 28(Suppl 1):38–42
40. Yiu JH, Dorweiler B, Woo CW (2017) Interaction between gut microbiota and toll-like receptor: from immunity to metabolism. *J Mol Med (Berl)* 95(1):13–20
41. Morales-Ibanez O, Dominguez M, Ki SH, Marcos M, Chaves JF, Nguyen-Khac E et al (2013) Human and experimental evidence supporting a role for osteopontin in alcoholic hepatitis. *Hepatology* 58(5):1742–1756
42. Anthony N, Foldi I, Hidalgo A (2018) Toll and Toll-like receptor signalling in development. *Development* 145(9)
43. Diehl KL, Vorac J, Hofmann K, Meiser P, Unterweger I, Kuerschner L et al (2020) Kupffer Cells Sense Free Fatty Acids and Regulate Hepatic Lipid Metabolism in High-Fat Diet and Inflammation. *Cells* 9(10):2258
44. Icer MA, Gezmen-Karadag M (2018) The multiple functions and mechanisms of osteopontin. *Clin Biochem* 59:17–24
45. Bruha R, Vitek L, Smid V (2020) Osteopontin - A potential biomarker of advanced liver disease. *Ann Hepatol* 19(4):344–352
46. Seth D, Duly A, Kuo PC, McCaughan GW, Haber PS (2014) Osteopontin is an important mediator of alcoholic liver disease via hepatic stellate cell activation. *World J Gastroenterol* 20(36):13088–13104
47. Lancha A, Rodriguez A, Catalan V, Becerril S, Sainz N, Ramirez B et al (2014) Osteopontin deletion prevents the development of obesity and hepatic steatosis via impaired adipose tissue matrix remodeling and reduced inflammation and fibrosis in adipose tissue and liver in mice. *PLoS One* 9(5):e98398
48. Ge X, Leung TM, Arriazu E, Lu Y, Urtasun R, Christensen B et al (2014) Osteopontin binding to lipopolysaccharide lowers tumor necrosis factor- α and prevents early alcohol-induced liver injury in mice. *Hepatology* 59(4):1600–1616
49. Arab JP, Roblero JP, Altamirano J, Bessone F, Chaves Araujo R, Higuera-De la Tijera F et al (2019) Alcohol-related liver disease: Clinical practice guidelines by the Latin American Association for the Study of the Liver (ALEH). *Ann Hepatol* 18(3):518–535
50. Singh S, Osna NA, Kharbanda KK (2017) Treatment options for alcoholic and non-alcoholic fatty liver disease: A review. *World J Gastroenterol* 23(36):6549–6570
51. Cederbaum AI (2012) Alcohol metabolism. *Clin Liver Dis* 16(4):667–685
52. Heier C, Taschler U, Radulovic M, Aschauer P, Eichmann TO, Grond S et al (2016) Monoacylglycerol Lipases Act as Evolutionarily Conserved Regulators of Non-oxidative Ethanol Metabolism. *J Biol Chem* 291(22):11865–11875
53. Maenhout TM, De Buyzere ML, Delanghe JR (2013) Non-oxidative ethanol metabolites as a measure of alcohol intake. *Clin Chim Acta* 415:322–329
54. Hugbart C, Verres Y, Le Dare B, Bucher S, Vene E, Bodin A et al (2020) Non-oxidative ethanol metabolism in human hepatic cells in vitro: Involvement of uridine diphospho-glucuronosyltransferase 1A9 in ethylglucuronide production. *Toxicol In Vitro* 66:104842
55. Donohue TM, Osna NA, Clemens DL (2006) Recombinant Hep G2 cells that express alcohol dehydrogenase and cytochrome P450 2E1 as a model of ethanol-elicited cytotoxicity. *Int J Biochem Cell Biol* 38(1):92–101
56. Osna NA, Clemens DL, Donohue TM Jr (2005) Ethanol metabolism alters interferon gamma signaling in recombinant HepG2 cells. *Hepatology* 42(5):1109–1117

Publisher's Note Springer Nature remains neutral with regard to jurisdictional claims in published maps and institutional affiliations.